Available online at www.sciencedirect.com
ScienceDirect
Journal of Hazardous Materials 153 (2008) 28–36
Journal of Hazardous Materials
www.elsevier.com/locate/jhazmat

Adsorption of Zn(II) in aqueous solution by activated carbons prepared from evergreen oak (*Quercus rotundifolia* L.)

M. del Mar Gómez-Tamayo [a], Antonio Macías-García [a], M. Angeles Díaz Díez [a], Eduardo M. Cuerda-Correa [b,*]

[a] *Department of Electronics and Electromechanical Engineering, Area of Materials Science, School of Industrial Engineering, University of Extremadura, Avda. de Elvas, s/n, E-06071 Badajoz, Spain*
[b] *Department of Inorganic Chemistry, Faculty of Sciences, University of Extremadura, Avda. de Elvas, s/n, E-06071 Badajoz, Spain*

Received 31 August 2006; received in revised form 16 June 2007; accepted 8 August 2007
Available online 11 August 2007

Abstract

In the present work activated carbons have been prepared from evergreen oak wood. Different samples have been prepared varying the concentration of the activating agent (H_3PO_4) and the treatment temperature. The yield of the process decreases with increasing phosphoric acid concentrations. Furthermore, high concentrations of activating agent lead to mainly mesoporous activated carbons to the detriment of the microporous texture. Treatment temperatures up to 450 °C lead to a progressive increase of the micro- and mesopore volumes. Values of specific surface area (S_{BET}) as high as 1723 $m^2\,g^{-1}$ have been obtained using appropriate phosphoric acid concentrations and treatment temperatures. The samples prepared have been successfully used in the removal of Zn(II) from aqueous solutions. From the adsorption kinetic data it may be stated that the equilibrium time is, in all cases, below 170 h. The adsorption process as a rule becomes faster as the mesopore volume and specific surface area of the samples increase. The adsorption isotherms in liquid phase point out that the adsorption capacity (n_0^s) and the affinity towards the solute (K_{ci}) are higher for the sample showing the most developed mesoporous texture and surface area as well.

Keywords: Activated carbon; Evergreen oak; Phosphoric acid activation; Zinc removal; Adsorption in liquid phase

1. Introduction

Evergreen oak (*Quercus rotundifolia* L.) is a Mediterranean medium-size tree that may reach up to 20–27 m tall. The flowers are catkins, produced in the spring whereas the fruit is an acorn, which matures in about 6 months. The acorns are an important food for free-range pigs reared for the food industry in the SW of Spain. The wood is hard and tough. As a consequence, it has been traditionally used for general construction purposes, firewood, and charcoal manufacture. In this connection, the charcoal has been recently used as the raw material for the preparation of activated carbons [1].

On the other hand, due to their accumulation through food chain and persistence in nature, ecotoxicological effects of heavy metals are a major concern nowadays [2]. Since levels of heavy metals in the environment have increased because of the industrial pollution [3,4], the elimination of such ions from water is essential to protect public health. In addition, these toxic elements can seriously affect plants and animals, causing a large number of afflictions. As a consequence, the setting up of experimental methods that enable the most rapid and efficient removal of heavy metals from a contaminated medium is of great importance, as pointed out by the great deal of attention received by this topic in the recent years (see [5] and references therein).

Trace amounts of zinc are essential for life. However, in large amounts zinc is a toxic element. Among the main symptoms of zinc toxicity, irritability, muscular stiffness, loss of appetite and nausea are to be mentioned [6]. A large excess of zinc may be carcinogenic [7]. The World Health Organization (WHO) recommends a level of zinc in drinking water below 5 $mg\,L^{-1}$ [8]. Zinc manufacturing and other industries such as pharmaceuticals, galvanizing, paints, pigments, insecticides, cosmetics, etc release large quantities of metals, mainly Cd and Zn, during production. Thus, up to 75% of the total amount of Zn released to

* Corresponding author.
E-mail address: emcc@unex.es (E.M. Cuerda-Correa).

0304-3894/$ – see front matter © 2007 Elsevier B.V. All rights reserved.
doi:10.1016/j.jhazmat.2007.08.012

the atmosphere yearly has its origin in human activities [9]. Consequently, the development of simple and effective experimental methods aimed to remove zinc from polluted environments as well as to reduce the release of zinc to the atmosphere is a topic of current interest [10–12].

The aim of this work was first to prepare and characterize activated carbons using a common by-product of the local agriculture such as evergreen oak wood as the raw material. Next, the feasibility of the activated carbons for Zn(II) removal from aqueous solution was tested with promising results.

2. Experimental

2.1. Preparation of the samples

The precursor used for the production of the activated carbons was evergreen oak wood from the trimming process of the tree. The raw material as received was crushed with the aid of a Grindomix GM200 knife mill. The sample was next sieved, the fraction of particle size below 1 mm being selected as the precursor. Then, the crushed wood was impregnated with solutions of different phosphoric acid concentration (namely, 15, 35, 60 and 85%) prepared from a commercial solution (85%, Carlo Erba). The impregnation temperature was 85 °C and the sample was kept in contact with the impregnating agent for 2 h under agitation at 80 rpm. The impregnated samples were next dried overnight in an oven at 120 °C and stored in a dessicator.

For the carbonization of the impregnated samples a Termolab tubular furnace equipped with Eurotherm 904 temperature controllers and a 1 m long tubular ceramic insert was used. The temperature within the furnace was first calibrated and the length and position of the constant temperature hot zone determined. About 15 g of each sample were placed in a stainless steel boat with perforated ends to facilitate gas flow and positioned in the center of the constant temperature zone. The carbonization of the samples was carried out at 400 °C. The heating rate was 10 °C min^{-1} under a constant N_2 flow of 200 cm^3 min^{-1}. The isothermal carbonization time was 2 h. Once this time was elapsed, the reactor was cooled to room temperature under the same nitrogen flow.

In order to test the influence of the carbonization temperature, the sample showing optimal characteristics in terms of porosity and surface area (i.e., that impregnated with 60% H_3PO_4 solution) was carbonized not only at 400 °C but also at 350, 450 and 550 °C.

All samples were thoroughly washed after carbonization. The rinse of the carbonized samples was carried out with distilled water under vacuum until a final pH equal to 6. The absence of phosphate ions in solution was also tested by addition of barium nitrate. The resulting products were oven dried overnight and next kept in a tightly closed container.

Table 1 summarizes the nomenclature and preparation conditions of all the samples used in the present study together with their yield and ash content. For comparative purpose, a non-impregnated evergreen oak sample (here denoted as EC) was prepared as well.

2.2. Characterization of the samples

The samples were texturally characterized by gas adsorption (N_2, 77 K), mercury porosimetry and helium and mercury densities.

Adsorption isotherms of N_2 (N-48, Air Liquide, purity ≥ 99.998%) at 77 K were collected using an adsorption apparatus (Autosorb-1, Quantachrome). The samples were placed in a glass container and degassed at 10^{-3} Torr at 120 °C overnight prior to the adsorption measurements. From the adsorption isotherms, the micropore volume (V_{mi}) was derived by reading the volume adsorbed (V_{ad}) at $P/P^\circ = 0.1$ and the mesopore volume (V_{me}) by subtraction of V_{mi} from V_{ad} at $P/P^\circ = 0.95$, all pore volumes being expressed as liquid volumes. With comparative purpose, the micropore volume of the samples was calculated according to the method proposed by Dubinin and Radushkevich [13]. The specific surface area (S_{BET}) was calculated by applying the BET equation [14]. The micropore size distribution as well as the average pore size were calculated by using the density functional theory (DFT) method [15].

A Quantachrome porosimeter, Autoscan-60, was used to obtain the mercury intrusion curves. The values of surface tension and contact angle used in the computational program of the porosimeter were 0.480 N m^{-1} and 140°, respectively. From the Hg intrusion curves the macropore ($V_{ma\text{-}p}$) and mesopore ($V_{me\text{-}p}$) volumes were calculated. Thus, $V_{ma\text{-}p}$ was considered to be the cumulative pore volume (CPV) corresponding to a pore radius equal to 250 Å, whereas $V_{me\text{-}p}$ was determined by the difference between the CPV obtained at the maximum pressure here applied and $V_{ma\text{-}p}$. The mercury density (ρ_{Hg}) was determined when effecting the mercury porosimetry. The volume of sample was obtained by knowing the calibration volume of the sample

Table 1
Nomenclature, preparation conditions, yield and ash content of the evergreen oak samples

Sample	H_3PO_4 concentration (%)	Carbonization temperature (°C)	Yield (%)	Ash content (%)
EC	–	400	79.4	5.48
E-15-400	15	400	48.9	3.87
E-35-400	35	400	39.8	3.04
E-60-400	60	400	30.4	1.09
E-85-400	85	400	28.6	0.90
E-60-350	60	350	29.9	1.02
E-60-450	60	450	28.8	3.12
E-60-550	60	550	28.6	4.32

holder and from the density of mercury at the working temperature. The helium density (ρ_{He}, N-50, Air Liquide) was measured using a Quantachrome stereopycnometer. From the values of ρ_{Hg} and ρ_{He}, the total pore volume (V_T) was determined by applying the following expression:

$$V_T = \frac{1}{\rho_{Hg}} - \frac{1}{\rho_{He}} \quad (1)$$

2.3. Adsorption of Zn(II) in aqueous solution

Only the samples showing optimal textural properties were used as adsorbents for the adsorption kinetic and equilibrium study in the liquid phase. The aqueous solutions of Zn(II) ion used in the adsorption process were prepared from Zn(II) chloride (Merck, proanalysis reagent) and deionized, bidistilled water.

The procedure used to carry out the adsorption kinetic experiments involved placing 0.1 g of sample in a series of 50 mL glass flasks furnished with threaded caps and adding 25 mL of a Zn(II) chloride solution of known concentration. The flasks were then stirred at 50 rpm at 25 ± 0.1 °C in an Unitronic-Orbital C shaker for different preset time intervals, after which the Zn(II) concentration in solution was determined with the aid of a Perkin-Elmer 370 atomic absorption spectrophotometer at 213.9 nm.

The equilibrium isotherms were determined similarly, using an amount of sample comprised between 0.01 and 1.00 g and 25 mL of an aqueous solution of Zn(II) of perfectly known concentration at a temperature of 25 °C under a 50 rpm stirring. The solid and liquid phases were kept in contact for a much longer time than that strictly needed for equilibrium to be reached.

In order to test the influence of pH on the adsorption of Zn^{2+}, adsorption experiments were performed at three pH values, namely at unmodified solution pH and at pH 2 and 12. These latter pH values were fixed in the adsorptive solution by adding concentrated HCl or NH_4OH solution.

3. Results and discussion

3.1. Preparation of the samples

Table 1 clearly shows that the yield of the samples decreases markedly as the concentration of the phosphoric acid solution increases. The yield of the samples prepared using different H_3PO_4 concentrations ranges between 48.9% for sample E-15-400 and 28.6% for sample E-85-400. On the contrary, the variation of the heat treatment temperature does not exert any remarkable effect on the yield of the samples. Table 1 shows that the yield in this latter case varies between 30.4% for sample E-60-400 and 28.6% for sample E-60-550. Consequently, these results suggest that, at least in the temperature range here studied, the interaction between the activating agent and the raw material takes place in a similar extension regardless what the treatment temperature is.

On the other hand, the referred table summarizes the ash content of the different samples. It may be observed that this parameter follows the same variation pattern that the yield for samples prepared varying the H_3PO_4 concentration (i.e., the ash content decreases with increasing H_3PO_4 concentration). The lowest ash contents correspond to samples E-60-400 and E-85-400. This fact suggests that the demineralizing effect is more remarkable as the phosphoric acid concentration increases. The catalytic effect of the ashes has been widely studied in the literature [16–21]. However, different conclusions may be withdrawn from a literature review. Thus, for some authors (as, for instance Salvador et al. [22] or Maldonado-Hodar et al. [23]) the ash content exerts a positive effect on the carbonization processes due to its catalytic effect. On the contrary, Linares-Solano et al. [24] and Vamvuka et al. [25] indicate that high ash contents may have a negative influence, reducing the rate of the reactions involved in this kind of processes. If the activated carbons obtained are aimed to the removal of ions from aqueous solutions – as is the case in the present study – our previous experience indicates that low ash contents are more effective and thus preferred [27–29]. Finally, Table 1 also shows that the ash content, as expected, increases with the treatment temperature.

3.2. Characterization of the samples

The N_2 adsorption isotherms obtained for the different samples are depicted in Fig. 1. From the shape of such isotherms it may be concluded that sample EC is a virtually non porous solid. The isotherms corresponding to samples EC-15-400 and EC-35-400 belong to the type I of the BDDT classification [26]. This kind of isotherms is typical of microporous solids for which the adsorption does not increase continuously, but reaches a limiting value at low relative pressure values. This causes the presence of a plateau corresponding to the maximum volume of nitrogen adsorbed. Furthermore, the shape of the isotherm corresponding to sample E-35-400 shows a more open knee than that of sample E-15-400. This fact suggests the presence of a wide variety of micropore sizes. This assertion will be corroborated by the application of the DFT model as it will be further discussed below. On the other hand, the adsorption isotherms of samples E-60-400 and E-85-400 belong to the type IV of the referred BDDT classification. This kind of isotherms is characteristic of mesoporous solids and shows an increased adsorption of nitrogen at relative pressure values close to one due to capillary condensation phenomena. It is worth noting that the opening of the knee is more noticeable as the H_3PO_4concentration increases.

For samples prepared varying the thermal treatment temperature (Fig. 1, right) it may be observed that this parameter strongly influences the development of micro- and mesoporosity. In all cases, and especially for sample E-60-450, the volume of nitrogen adsorbed is larger than that adsorbed by the corresponding precursor.

Table 2 summarizes the textural parameters calculated as described in the previous section. From the results obtained it may be observed that the concentration of phosphoric acid exerts a remarkable influence on the development of the micro- and mesoporous texture of the samples. Thus, sample E-35-400 shows the most developed microporous texture, whereas the most mesoporous sample among those prepared varying the concentration of H_3PO_4 is EC-85-400. It is also inter-

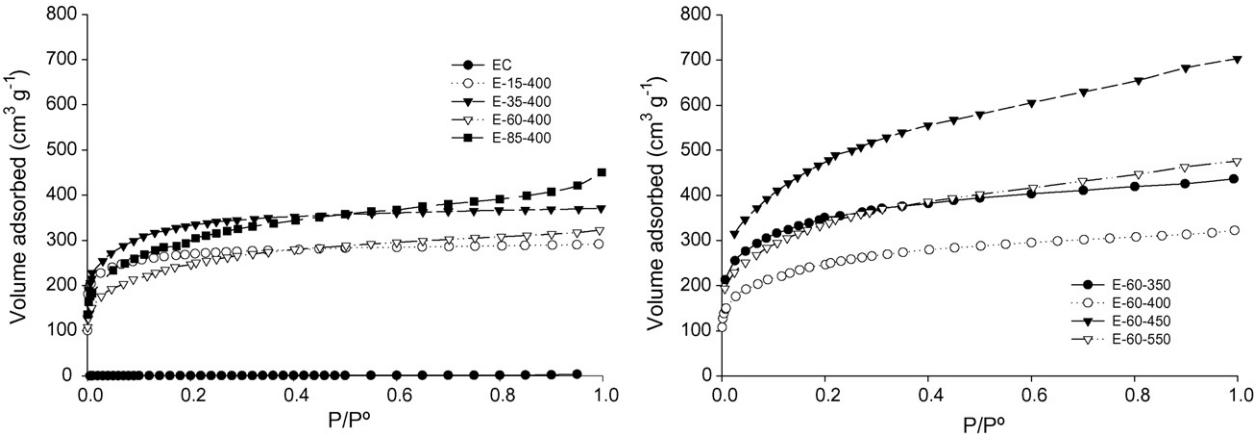

Fig. 1. Nitrogen adsorption isotherms of the samples prepared varying the phosphoric acid concentration (left) and the treatment temperature (right).

esting to point out the good agreement between the values of the micropore volumes calculated directly by reading the adsorption isotherms (V_{mi}) and those obtained by applying the Dubinin–Radushkevich equation (W_0). Furthermore, the chemical activation process by impregnation with phosphoric acid leads to a highly developed surface area, reaching values as high as 1217 $m^2\ g^{-1}$ for sample E-35-400.

With respect to the samples prepared varying the treatment temperature, the best of all the samples prepared in this study is E-60-450. This sample shows excellent porous development and surface area, which is worth noting. The values of micro- and mesopore volumes, as well as those of specific surface area are higher than those previously reported in the literature for other lignocellulosic materials prepared by phosphoric acid activation, even at higher thermal treatment temperatures [30–33].

The mercury intrusion curves corresponding to the different samples are depicted in Fig. 2. This figure indicates that sample EC possesses mainly wide pores (macropores) and lacks of narrow mesopores since the initial portion of the plot is nearly flat. The samples prepared using different concentrations of phosphoric acid possess well developed meso- and macropores. As a rule, the slope of the plots is more pronounced at low values of radius. This fact indicates that the variation in the pore sizes is more remarkable in the mesopore region. The samples prepared at different treatment temperatures show, in all cases, a wide range of pores of different sizes. This fact points out the significant influence of the treatment temperature on the development of the mesoporous texture. It may be concluded that an increase in the phosphoric acid concentration involves the development of macropores whereas a growth of the carbonization temperature up to 450 °C leads to a more developed mesoporous texture. These assertions are corroborated from the values of $V_{me\text{-}p}$ and $V_{ma\text{-}p}$ included in Table 2. Thus, among the samples prepared varying the H_3PO_4concentration, sample E-85-400 presents the most developed macroporous texture and sample E-60-400 exhibits the largest value of mesopore volumes.

Table 2 also summarizes the total pore volumes calculated from the helium and mercury densities. In general, the values of V_T are large, the samples hence showing a well developed porosity.

On the other hand, the DFT plots depicted in Fig. 3 corroborate the facts pointed out by the shapes of the adsorption isotherms. From the DFT plots corresponding to the samples prepared varying the phosphoric acid concentration (Fig. 3, left) it may be observed that sample EC is virtually non porous. Furthermore, sample E-15-400 shows a single peak in the DFT plot centered at 10 Å, whereas two peaks centered at 11 and 15 Å are shown by sample E-35-400. Thus, it may be stated that this latter sample possesses a wider variety of micropore

Table 2
Textural properties of the activated carbons

Sample	V_{mi} ($cm^3\ g^{-1}$)	V_{me} ($cm^3\ g^{-1}$)	W_0 ($cm^3\ g^{-1}$)	S_{BET} ($m^2\ g^{-1}$)	APS (Å)	$V_{ma\text{-}p}$ ($cm^3\ g^{-1}$)	$V_{me\text{-}p}$ ($cm^3\ g^{-1}$)	ρ_{He} ($g\ cm^{-3}$)	ρ_{Hg} ($g\ cm^{-3}$)	V_T ($cm^3\ g^{-1}$)
EC	0.001	0.005	0.001	2.8	14.09	0.530	0.070	1.24	0.72	0.580
E-15-400	0.398	0.051	0.365	1011	10.28	0.320	0.200	1.56	0.63	0.940
E-35-400	0.477	0.095	0.431	1217	11.24	0.120	0.230	1.66	0.76	0.710
E-60-400	0.337	0.154	0.296	866	11.76	0.200	0.300	1.62	0.72	0.770
E-85-400	0.407	0.244	0.351	1066	11.24	0.630	0.180	1.61	0.44	1.650
E-60-350	0.489	0.176	0.540	1245	12.30	0.190	0.350	1.60	0.71	0.780
E-60-450	0.631	0.439	0.706	1723	14.73	0.330	0.610	1.84	0.47	1.580
E-60-550	0.455	0.272	0.507	1217	12.30	0.110	0.420	1.85	0.67	0.950

The textural data were obtained from the N_2 adsorption isotherms at 77 K: S_{BET} ($P/P^\circ = 0.05$–0.35, $a_m = 16.2$ Å), V_{mi} (volume adsorbed, V_{ad}, at $P/P^\circ = 0.10$), V_{me} (V_{ad} at $P/P^\circ = 0.95$ to V_{ad} at $P/P^\circ = 0.10$), and W_0 (Dubinin–Radushkevich equation); mercury intrusion curves: $V_{me\text{-}p}$, $V_{ma\text{-}p}$; the helium and mercury density values (ρ_{He} and ρ_{Hg}): $V_T = 1/\rho_{Hg} - 1/\rho_{He}$. V_{mi}, V_{me} and W_0 are expressed as liquid volumes.

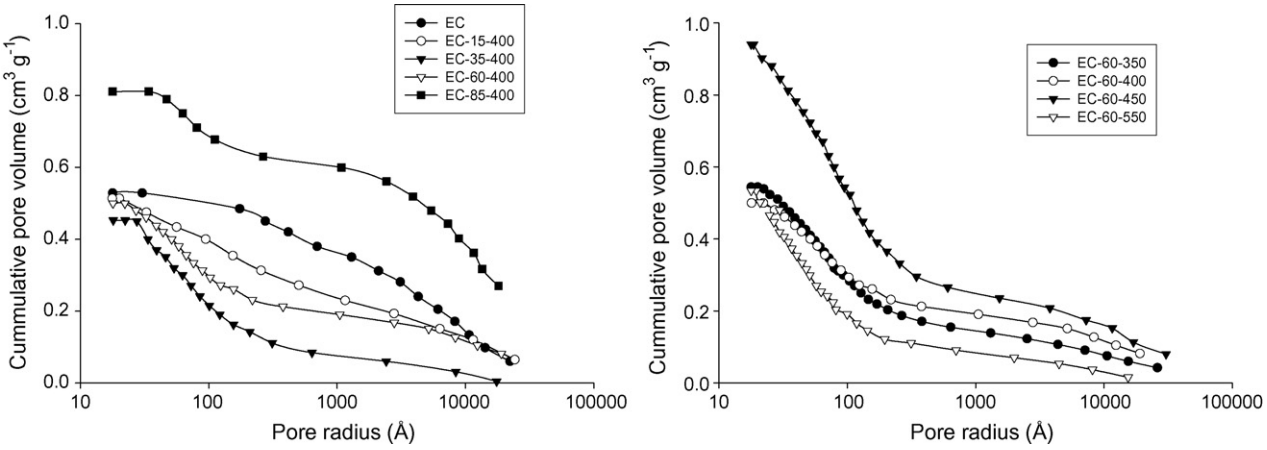

Fig. 2. Mercury intrusion curves of the samples prepared varying the phosphoric acid concentration (left) and the treatment temperature (right).

sizes as suggested by the opening of the knee in the adsorption isotherm. As indicated above, samples E-60-400 and E-85-400 are mainly mesoporous samples, both presenting a peak centered at approximately 25 Å.

With respect to samples prepared using different treatment temperatures (Fig. 3, right) as suggested by the adsorption isotherms the porous texture is developed to a larger extent. Moreover, a great variety of pore sizes in micro- and mesopore regions is observed, especially for sample E-60-450. This fact, together with the data summarized in Table 2, confirms that this sample shows the best textural characteristics among all the samples here reported.

For comparative purpose, the most relevant results previously reported in the literature using different species of *Quercus* as the raw material for the preparation of activated carbons have been included in Table 3.

It is worth noting that samples prepared in this study, mainly E-60-450, show very high values of V_{me} when compared with those summarized in Table 3. Thus, for instance, Figueroa-Torres et al. [34] have prepared samples with extremely large sepecific surface area (S_{BET} values as high as 3081 $m^2\,g^{-1}$) using KOH as the activating agent. However, such values of S_{BET} are obtained to the detriment of those of V_{me}, that reach only 0.091 $cm^3\,g^{-1}$. As a consequence, it may be stated that these samples will not show a good behavior in terms of adsorption of solutes in the liquid phase. For this purpose, adsorbents with larger V_{me} values are strongly preferred, as it will be discussed below. With respect to the remainig works, the samples prepared in this study are, in general, better than those summarized in Table 3, both in terms of specific surface area and pore volumes.

3.3. Adsorption of Zn(II) in aqueous solution

3.3.1. Study of the adsorption kinetics

As indicated above, only the samples showing optimal textural properties were used as adsorbents in the liquid phase. The initial concentration of Zn^{2+}in the aqueous solution was 10^{-4} M. This initial concentration, which is equivalent to 13.64 mg L^{-1}, is almost three times larger than the concentration recommended by the WHO as indicated in the Introduction. The samples used were E-35-400, E-85-400. E-60-350 and E-60-450.

A method previously described by the authors [37,38] has been used here in order to analyze the kinetic data. Thus, the following equation has been applied to the experimental results:

$$C = \frac{C_0 + k_a \cdot C_e \cdot t}{1 + k_a \cdot t} \quad (2)$$

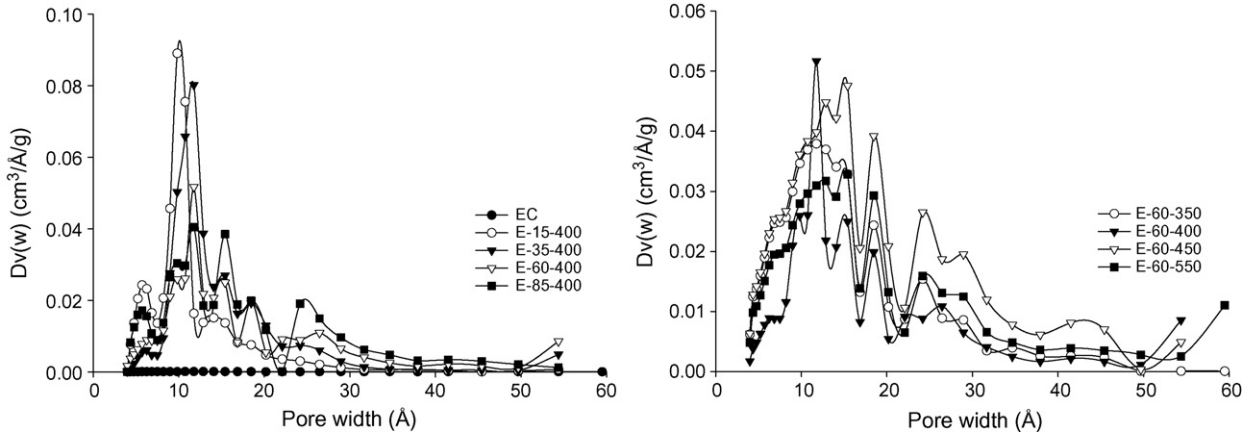

Fig. 3. DFT curves of the samples prepared varying the phosphoric acid concentration (left) and the treatment temperature (right).

Table 3
Textural properties of activated carbons prepared using different species of *Quercus* as the raw material

Author(s)	Reference	Raw material	Activating agent	S_{BET} ($m^2\ g^{-1}$)	V_{mi} ($cm^3\ g^{-1}$)	V_{me} ($cm^3\ g^{-1}$)	V_T ($cm^3\ g^{-1}$)
Figueroa-Torres et al.	[34]	*Quercus agrifolia*	KOH	1393–3081	0.67–1.43	0.008–0.091	0.68–1.52
			NaOH	1019–2252	0.43 –0.95	0.09–0.31	0.52–1.27
Macías-García et al.	[1]	*Quercus rotundifolia*	CO_2	523–1110	0.231 –0.415	0.04–0.129	0.66–0.77
			Steam	420–987	0.202 –0.403	0.026–0.182	0.59–0.71
			CO_2/steam	705–885	0.289 –0.340	0.084–0.107	0.73–0.88
Jagtoyen and Derbyshire	[35]	*Quercus alba*	H_3PO_4	n.a.	0.11 –0.68	0.03–0.55	n.a.
Zhang et al.	[36]	*Quercus* sp.	CO_2	642–985	0.245 –0.379	n.a.	0.534–0.657

n.a., not available.

Table 4
Adsorption specific rates and equilibrium times of the adsorption process of Zn(II) on the selected activated carbons

Sample	k_a (h^{-1})	R^2	t_e (h)
E-35-400	0.1281	0.9253	168
E-85-400	0.1657	0.9768	98
E-60-350	0.1456	0.9392	166
E-60-450	0.2319	0.9917	109
E-60-450 (pH 12)	0.5686	0.9944	72

where C_0 is the initial Zn(II) concentration in solution (mol L^{-1}), k_a the adsorption specific rate (h^{-1}), C_e the Zn(II) concentration in solution at equilibrium time (mol L^{-1}) and t is the time (h).

The values of the adsorption specific rates calculated by applying this equation to the experimental kinetic data, together with the corresponding equilibrium times (te) are summarized in Table 4.

The variation of the initial concentration of the Zn(II) solutions in contact with the adsorbent versus time is depicted in Fig. 4. The solid lines in these plots represent the theoretical values of the C versus t curves calculated using the fitting parameter obtained from Eq. (2). In all cases a good agreement has been found between the experimental and calculated data. From the C versus t plot it may be concluded that most of the Zn(II) adsorption takes place at values of time below 100 h approximately. Once elapsed this period of time, the adsorption kinetics becomes slower until the equilibrium time is reached. Furthermore, the slope of the initial tract of the curves depicted in Fig. 4 suggests that the rate of the adsorption process varies according to the following trend: $E-60-450 \geq E-60-350 \geq E-85-400 \geq E-35-400$. This assertion is corroborated from the numerical values of k_a summarized in Table 4. It may be concluded that the adsorption kinetics of Zn(II) is strongly influenced by the pore size distribution of the solid adsorbents here used. In fact, the pore size distribution appears to be the main factor governing the easiness of the access of the solute to the active sites of the adsorbent. In this case, since the Zn(II) ions are adsorbed in an at least partially solvated manner, mesoporosity exerts a noticeable influence on the adsorption kinetics. Thus, as a rule, the larger the mesopore volume (V_{me}, see Table 2) the faster the adsorption process will be. As expected, the values of the specific surface area (S_{BET}) also play an important role in this connection. Hence, as the value of S_{BET} increases the adsorption process becomes faster as well.

3.3.2. Study of the adsorption equilibrium

The adsorption isotherms measured for the different samples are plotted in Fig. 5. All of them belong to the L-type of the

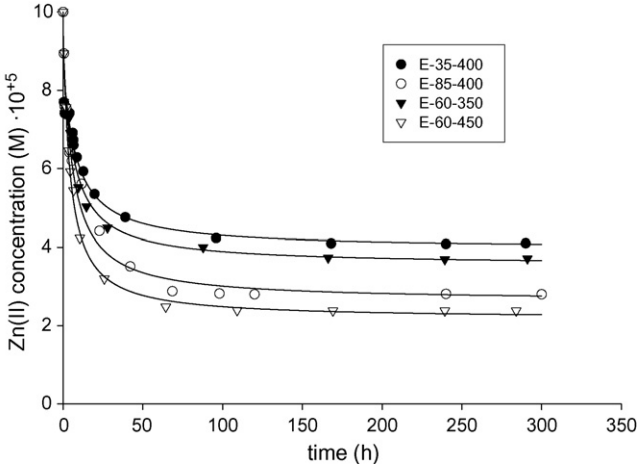

Fig. 4. Adsorption kinetics of Zn(II) from aqueous solution.

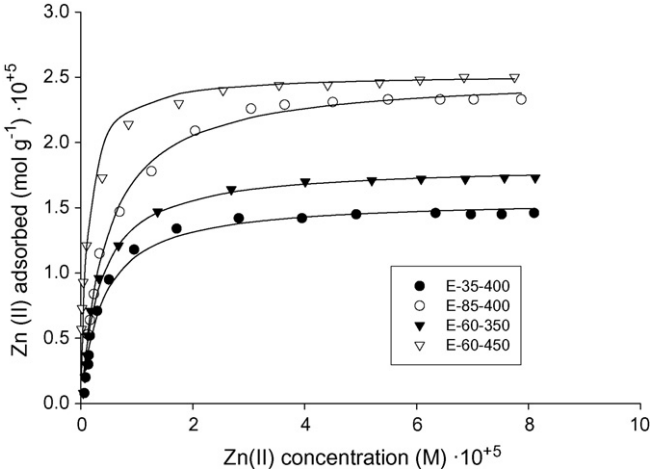

Fig. 5. Adsorption isotherms of Zn(II) from aqueous solution.

classification proposed by Giles [39]. Such type of isotherms may be fitted to the Langmuir equation:

$$n^s = \frac{n_0^s \cdot K_{ci} \cdot C_e}{1 + K_{ci} \cdot C_e} \quad (3)$$

or, in linearized form:

$$\frac{C_e}{n^s} = \frac{1}{n_0^s \cdot K_{ci}} + \frac{C_e}{n_0^s} \quad (4)$$

Accordingly, the plot of the adsorption isotherm tends to an asymptotic value that corresponds to the adsorption capacity (n_0^s) and the slope of the initial segment of the isotherm is indicative of the affinity of the solute towards the active site of the adsorbent. Such affinity is mathematically expressed by the value of K_{ci}. Thus, large values of K_{ci} indicate high affinity of Zn(II) towards the active sites of the activated carbons. The values of n_0^s and K_{ci} corresponding to the fitting of the experimental data to Eq. (4) are summarized in Table 5. The solid lines in the plots of the adsorption isotherms in solution (Fig. 5) represent the theoretical values calculated using the fitting parameters obtained from Eq. (4). For comparative purposes the experimental data have been fitted to the well-known Freundlich equation:

$$n^s = K_f \cdot C^n \quad (5)$$

or, in linearized form:

$$\mathrm{Ln}\, n^s = \mathrm{Ln}\, K_f + n\, \mathrm{Ln}\, C \quad (6)$$

The fitting parameters corresponding to this latter equation have been reported in Table 5 as well. From the values of R^2 summarized in Table 5 it may be concluded that both equations fit reasonably well the experimental data, although the Langmuir equation provides a better fit than the Freundlich one.

According to the Langmuir parameters, the samples showing the largest adsorption capacities (n_0^s) are E-85-400 and E-60-450. However, the value of K_{ci}– and consequently, the affinity towards the solute – is larger for this latter sample. This fact corroborates that the sample showing optimal textural properties in terms of mesoporosity and surface area is also the best adsorbent to be used in the removal of Zn(II) from aqueous solution.

On the other hand, the application of the Freundlich equation makes it possible to calculate the dose of adsorbent (D) in gram per liter that is necessary for a total removal of the solute from the aqueous solution. The values of D calculated for the different Zn-activated carbon systems here studied have been included in Table 5. Such values confirm that, as suggested by the Langmuir parameters, the samples with the highest adsorption capacities (i.e., E-85-400 and E-60-450) will require the lowest dose (D) for a complete removal of the Zn(II) ions from the liquid phase. In fact, only 3.6 g of sample are necessary to remove all the Zn(II) dissolved in one liter of $ZnCl_2$ of initial concentration equal to 10^{-4} M (or 13.64 mg L^{-1}). This fact points out that evergreen oak wood is a promising raw material for the preparation of activated carbons aimed to the removal of Zn(II) ions from contaminated media.

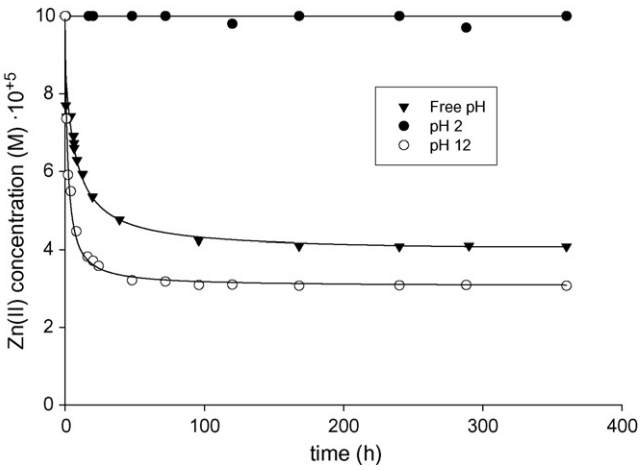

Fig. 6. Influence of pH on the adsorption kinetics of Zn(II) from aqueous solution.

3.3.3. Effect of pH on adsorption of Zn^{2+} onto the adsorbents

In order to study the influence of pH on the adsorption of Zn^{2+}, both kinetic and equilibrium experiments were performed at three pH values, namely, unmodified solution pH and pHs 2 and 12. Only the sample showing optimal adsorption properties (i.e., sample E-60-450) has been used as the adsorbent. The adsorption kinetics at such pHs are shown in Fig. 6. According to the plots included in this figure, the behavior is quite different depending on pH. Thus, whereas at pH 2 the adsorption of Zn^{2+} does not occur at all (as deducted from the fact that the corresponding plot is parallel to the abscissa axis in the whole t range), at pH 12 the extent of the process is large and it is faster than at unmodified solution pH. The same conclusion may be drawn from the values of k_a and t_e included in Table 4. The pH change in the adsorptive solution to 2 and 12 implies the incorporation of a large amount of protons or hydroxyl groups

Table 5
Fitting parameters to the Langmuir's and Freundlich's equations and adsorbent dose to complete removal of Zn

Sample	Langmuir equation			Freundlich equation			
	n_0^s ($\times 10^5$ mol g^{-1})	K_{ci} ($\times 10^{-5}$)	R^2	K_f ($\times 10^4$ L g^{-1})	n	R^2	D (g L^{-1})
E-35-400	1.56	2.63	0.9866	2.32	0.28	0.8654	5.8
E-85-400	2.51	2.23	0.9954	3.29	0.27	0.9119	3.6
E-60-350	1.82	2.97	0.9915	2.88	0.29	0.8956	4.9
E-60-450	2.52	8.98	0.9989	1.63	0.19	0.9788	3.6
E-60-450 (pH 12)	3.90	8.21	0.9982[a]	1.54	0.16	0.9239[a]	4.1

[a] *Note*. Only experimental data below $C = 5 \times 10^{-5}$ have been considered for Langmuir and Freundlich fitting in this case.

to the solution, respectively. As a consequence, the ionic content is much higher than for the solution at unmodified pH. This fact should favor the electrostatic interactions in the solution, thus hindering the displacement of the Zn^{2+}ions towards adsorbent surface so that the adsorption can occur. Therefore, the pH change should be expected to unfavor the adsorption process from the kinetic point of view. However, as discussed below, it is not necesarily so. The behavior observed at pH 2 denotes a strong competition effect between the Zn^{2+}ion and the H_3O^+ ion for the active sites of the adsorbent. As a result, the Zn^{2+} ion does not become adsorbed. A greatly decreased adsorption by effect of lowering pH also to 2 in the adsorptive solution was noted before when investigating the adsorption of a number of metal ions from aqueous solution by heat-treated and sulfurized activated carbon [40]. In this connection, it should be born in mind that the mobility of the H_3O^+ion in water is abnormally high as compared with most other ions [41]. Owing to this fact, therefore, the H_3O^+ion will compete favorably with any other ion present in the solution for the basic adsorption sites.

On the other hand, the much higher rate of adsorption at pH 12 must be associated with the presence of hydroxo-complexes in the adsorptive solution at this pH value. According to the literature [42], the chemical species of Zn^{2+}existing in the solution at pH 12 are mostly $Zn(OH)_2$, $Zn(OH)_3^-$and $Zn(OH)_4^{2-}$. Since such species possess a large size, their ionic potential is then lower and this should reduce the degree of electrostatic interaction with the other ions present in the adsorptive solution, namely OH^-. It should make easier the diffusion of $Zn(OH)_3^-$ and $Zn(OH)_4^{2-}$ in such a solution, speeding up the adsorption process. A relevant fact in connection with the adsorption of $Zn(OH)_3^-$ and $Zn(OH)_4^{2-}$ is that the OH^- in excess is also found in the adsorption medium when the adsorption of the species of Zn^{2+} occurs. Thus, $Zn(OH)_3^-$ and $Zn(OH)_4^{2-}$ adsorb in spite of the OH^- ion being a very mobile chemical species [41]. It may be related to the strength as a base of the various species present in the solution since, as a result, they may prefer to interact specifically with acidic surface centers of the adsorbent.

These assertions are corroborated from the equilibrium isotherms of Zn^{2+}on the solid sorbents depicted in Fig. 7. It may be observed that, as indicated by the kinetic experiments, the adsortion of Zn^{2+}at pH 2 does not take place at all due to the competitive effect between $H_3O^+$and Zn^{2+} ions. On the contrary, the adsorption at pH 12 takes place in a more extensive manner than at free pH, as pointed out by the values of n_0^s included in Table 5. Furthermore, the presence of a final branch of the isotherm showing a remarkable slope is attributable to the precipitation of $Zn(OH)_2$on the surface of the adsorbent.

Values of n_0^s and K_{ci} summarized in Table 5 indicate that, as expected, when the adsorption equilibrium isotherms were determined at pH 12 the adsorption capacity increased noticeably, due to a faster and more remarkable adsorption of $Zn(OH)_3^-$ and $Zn(OH)_4^{2-}$ species as well as to a precipitation of $Zn(OH)_2$ on the solid sorbent. However, Fig. 7 indicates that the slope of the initial portion of the isotherm at pH 12 is less pronounced than that at free pH. As a consequence, it may be stated that the affinity ot the chemical species in solution towards the active

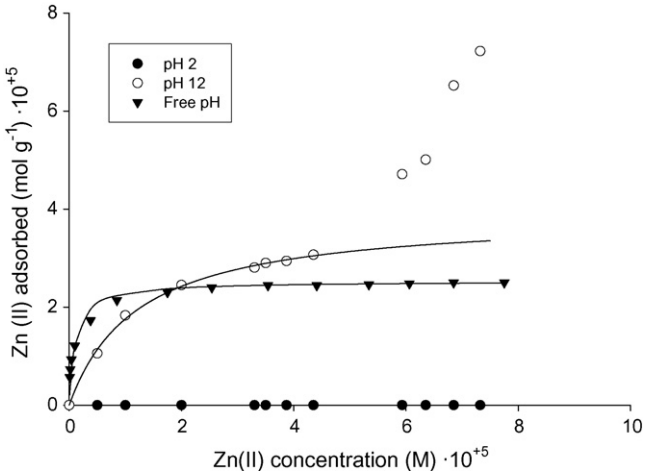

Fig. 7. Influence of pH on the adsorption equilibrium of Zn(II) from aqueous solution.

sites of the adsorbent is lower when pH increases up to 12. This assertion is corroborated from the values of K_{ci} summarized in Table 5 (i.e., 8.98 and 8.21×10^5 for free pH and pH 12, respectively).

4. Conclusions

Activated carbons have been prepared using evergreen oak wood as the raw material in order to remove Zn(II) ions from aqueous solutions. Samples have been prepared varying the concentration of the activating agent (H_3PO_4) and the treatment temperature. In this connection, the variation of the phosphoric acid concentration exerts a noticeable infuence on the yield of the process as well as on the porous texture of the samples. Thus, high concentrations of activating agent lead to low yields and mainly mesoporous activated carbons, whereas low concentrations of H_3PO_4 give rise to high yields of mainly microporous samples. On the other hand, the treatment temperature exerts a positive effect on the development of the micro- and mesoporous texture up to 450 °C. Higher treatment temperatures result in a decrease of the micro- and mesopore volumes.

The samples prepared have been successfully used in the removal of Zn(II) from aqueous solutions. The adsorption kinetics indicates that the equilibrium time is, in all cases, below 170 h, the adsorption process being in general faster as the mesopore volume and specific surface area of the samples increase. From the adsorption isotherms in liquid phase it may be concluded that the adsorption capacity (n_0^s) and the affinity towards the solute (K_{ci}) are higher for the sample showing a more developed mesoporous texture (i.e., sample E-60-450). If the kinetic experiments are carried out at strongly acidic pH, the adsorption of Zn(II) is remarkably hindered, whereas in basic solution such adsorption is accelerated and occurs in a more extensive manner. The values of D obtained by application of the Freundlich equation (especially those corresponding to samples E-85-400 and E-60-450) point out that evergreen oak wood is a promising raw material for the preparation of activated carbons aimed to the removal of Zn(II) ions from contaminated media.

References

[1] A. Macías-García, M.J. Bernalte-Garcia, M.A. Díaz Díez, A. Hernandez-Jimenez, Preparation of active carbons from a commercial holm-oak charcoal: study of micro- and meso-porosity, Wood Sci. Technol. 37 (2004) 385–394.

[2] A.K. Bhattacharya, S.N. Mandal, S.K. Das, Adsorption of Zn(II) from aqueous solution by using different adsorbents, Chem. Eng. J. 123 (2006) 43–51.

[3] K. Periasamy, C. Namasivayam, Process development for removal and recovery of cadmium from waste-water by a low-cost adsorbent: adsorption rates and equilibrium studies, Ind. Eng. Chem. Res. 33 (1994) 317–320.

[4] K. Periasamy, C. Namasivayam, Adsorption of Pb(II) by peanut hull carbon from aqueous solutions, Sep. Sci. Technol. 30 (1995) 2223–2237.

[5] S. Babel, T.A. Kurniawan, Low-cost adsorbents for heavy metals uptake from contaminated water: a review, J. Hazard. Mater. B97 (2003) 219–243.

[6] W. Kaim, B. Schwederski, Bioinorganic Chemistry: Inorganic Elements in the Chemistry of Life. An Introduction and Guide, John Wiley and Sons, 2001, p. 242.

[7] J. Emsley, The Elements, Oxford University Press, Oxford, 1989, p. 213.

[8] World Health Organization (WHO), Guidelines for Drinking Water Quality, vol. 1, 1993, p. 52.

[9] X. Domenech, Atmospheric Chemistry. Origin and Effects of Pollution, Miraguano Ediciones, Madrid, 1995, p. 57.

[10] R. Leyva Ramos, L.A. Bernal Jacome, J. Mendoza Barron, L. Fuentes Rubio, R.M. Guerrero Coronado, Adsorption of zinc(II) from an aqueous solution onto activated carbon, J. Hazard. Mater. B90 (2002) 27–38.

[11] Y.H. Wang, S.H. Lin, R.S. Juang, Removal of heavy metal ions from aqueous solutions using various low-cost adsorbents, J. Hazard. Mater. B102 (2003) 291–302.

[12] D. Mohan, K.P. Singh, Single- and multi-component adsorption of cadmium and zinc using activated carbon derived from bagasse—an agricultural waste, Water Res. 36 (2002) 2304–2318.

[13] M.M. Dubinin, L.V. Radushkevich, Equation of the characteristic curve of activated charcoal, Proc. Acad. Sci. USSR 55 (1947) 331–333.

[14] S. Brunauer, P.H. Emmett, E. Teller, Adsorption of gases in multimolecular layers, J. Am. Chem. Soc. 60 (1938) 309–319.

[15] R. Evans, U.M.B. Marconi, P. Tarazona, Fluids in narrow pores: adsorption, capillary condensation, and critical points, J. Chem. Phys. 84 (1986) 2376–2799.

[16] D.P. Ye, J.B. Agnew, D.K. Zhang, Gasification of a South Australian low-rank coal with carbon dioxide and steam: kinetics and reactivity studies, Fuel 77 (1998) 1209–1219.

[17] Z. Wua, Y. Sugimoto, H. Kawashima, Effect of demineralization and catalyst addition on N_2 formation during coal pyrolysis and on char gasification, Fuel 82 (2003) 2057–2064.

[18] P. Samaras, E. Diamadopoulos, G.P. Sakellaropoulos, The effect of mineral matter and pyrolysis conditions on the gasification of Greek lignite by carbon dioxide, Fuel 75 (1996) 1108–1114.

[19] D. Erincin, A. Sinag, Z. Misirlioglu, M. Canel, Characterization of burning and CO_2 gasification of chars from mixtures of Zonguldak (Turkey) and Australian bituminous coals, Energy Conver. Manage. 46 (2005) 2748–2761.

[20] J.M. Encinar, J.F. Gonzalez, J.J. Rodriguez, M.J. Ramiro, Catalysed and uncatalysed steam gasification of eucalyptus char: influence of variables and kinetic study, Fuel 80 (2001) 2025–2036.

[21] E. Iniesta, F. Sanchez, A.N. Garcia, A. Marcilla, Yields CO_2 reactivity of chars from almond shells obtained by a two heating step carbonisation process. Effect of different chemical pre-treatments and ash content, J. Anal. Appl. Pyrol. 58–59 (2001) 983–994.

[22] S. Salvador, J.M. Commandre, B.R. Stanmore, Reaction rates for the oxidation of highly sulphurised petroleum cokes: the influence of thermogravimetric conditions and some coke properties, Fuel 82 (2003) 715–720.

[23] F.J. Maldonado-Hodar, L.M. Madeira, M.F. Portela, The use of coals as catalysts for the oxidative dehydrogenation of *n*-butane, Appl. Catal. A: Gen. 178 (1999) 49–60.

[24] A. Linares-Solano, I. Martin-Gullon, C.S.-M. de Lecea, B. Serrano-Talavera, Activated carbons from bituminous coal: effect of mineral matter content, Fuel 79 (2000) 635–643.

[25] D. Vamvuka, S. Troulinos, E. Kastanaki, The effect of mineral matter on the physical and chemical activation of low rank coal and biomass materials, Fuel 85 (2006) 1763–1771.

[26] S. Brunauer, L.S. Deming, W.S. Deming, E. Teller, On the theory of Van der Waals adsorption of gases, J. Am. Chem. Soc. 62 (1940) 1723–1732.

[27] E. Manchon-Vizuete, A. Macías-García, A. Nadal Gisbert, C. Fernandez-Gonzalez, V. Gomez-Serrano, Adsorption of mercury by carbonaceous adsorbents prepared from rubber of tyre wastes, J. Hazard. Mater. 119 (2005) 231–238.

[28] A. Macías-García, C. Valenzuela-Calahorro, A. Espinosa-Mansilla, A. Bernalte-Garcia, V. Gomez-Serrano, Adsorption of Pb^{2+} in aqueous solution by SO_2-treated activated carbon, Carbon 42 (2004) 1755–1764.

[29] A. Macías-García, V. Gomez-Serrano, M.F. Alexandre-Franco, C. Valenzuela-Calahorro, Adsorption of cadmium by sulphur dioxide treated activated carbon, J. Hazard. Mater. 103 (2003) 141–152.

[30] B. Corcho-Corral, M. Olivares-Marn, E. Valdes-Sanchez, C. Fernandez-Gonzalez, A. Macías-García, V. Gomez-Serrano, Development of activated carbon using vine shoots (*Vitis vinifera*) and its use for wine treatment, J. Agric. Food Chem. 53 (2005) 644–650.

[31] J.A.F. MacDonald, D.F. Quinn, Adsorbents for methane storage made by phosphoric acid activation of peach pits, Carbon 34 (1996) 1103–1108.

[32] F. Carrasco-Marin, M.A. Alvarez-Merino, C. Moreno-Castilla, Microporous activated carbons from a bituminous coal, Fuel 75 (1996) 966–970.

[33] F. Suarez-Garcia, A. Martinez-Alonso, J.M.D. Tascon, Pyrolysis of apple pulp: chemical activation with phosphoric acid, J. Anal. Appl. Pyrol. 63 (2002) 283–301.

[34] M.Z. Figueroa-Torres, A. Robau-Sachez, L. De la Torre-Sanz, A. Aguilar-Elguezabal, Hydrogen adsorption by nanostructured carbons synthesized by chemical activation, Micropor. Mesopor. Mater. 98 (2007) 89–93.

[35] M. Jagtoyen, F. Derbyshire, Activated carbons from yellow poplar and white oak by H_3PO_4 activation, Carbon 36 (1998) 1085–1097.

[36] T. Zhang, W.P. Walawender, L.T. Fan, M. Fan, D. Daugaard, R.C. Brown, Preparation of activated carbon from forest and agricultural residues through CO_2 activation, Chem. Eng. J. 105 (2004) 53–59.

[37] C. Valenzuela-Calahorro, E. Cuerda-Correa, A. Navarrete-Guijosa, E. Gonzalez Pradas, Application of a single model to study the adsorption kinetics of prednisolone on six carbonaceous materials, J. Colloid Interf. Sci. 248 (2002) 33–40.

[38] R. Pardo-Botello, C. Fernandez-Gonzalez, E. Pinilla-Gil, E.M. Cuerda-Correa, V. Gomez-Serrano, Adsorption kinetics of zinc in multicomponent ionic systems, J. Colloid Interf. Sci. 277 (2004) 292–298.

[39] C.H. Giles, D. Smith, A. Huitson, General treatment and classification of the solute adsorption isotherm. I. Theoretical, J. Colloid Interf. Sci. 47 (1974) 755–765.

[40] V. Gomez-Serrano, A. Macías-García, A. Espinosa-Mansilla, C. Valenzuela-Calahorro, Adsorption of mercury, cadmium and lead from aqueous solution on heat-treated and sulphurized activated carbon, Water Res. 1 (1998) 1–4.

[41] N.-N. Greenwood, A. Earnshaw, Chemistry of the Elements, Pergamon Press, Oxford, 1989.

[42] C.-F. Baes, R.-E. Mesmer, The Hydrolysis of Cations, John Wiley & sons, New York, 1976.